Contribution from the Department of Chemistry, Thimann Laboratories, University of California, Santa Cruz, California 95064, and Department of Chemistry and Biochemistry, University of Windsor, Windsor, Ontario, Canada N9B 3P4

Syntheses, Structures, and Spectral Properties of a Synthetic Analogue of Copper(II)-Bleomycin and an Intermediate in the Process of Its Formation

Steven J. Brown, Samuel E. Hudson, Douglas W. Stephan,† and Pradip K. Mascharak*

Received July 22, 1988

As part of the systematic synthetic analogue approach to metallobleomycins (M-BLMs), a major portion of the metal-chelating locus of the antitumor drug bleomycin (BLM) has been synthesized. Unlike all the synthetic analogues reported previously, the present one, abbreviated as PMAH (**2**), contains a pyrimidine ring in the organic framework. The structure of the copper(II) complex of PMAH has been determined by X-ray crystallography. The complex $[Cu(PMA)]ClO_4 \cdot 0.5H_2O \cdot 0.5CH_3OH$ (**3b**) crystallizes in the orthorhombic space group *Pbca* with $a = 14.934$ (6) Å, $b = 15.617$ (8) Å, $c = 17.856$ (8) Å, $V = 4164$ (3) Å^3, and $Z = 8$. The structure of **3b** was refined to $R = 5.84\%$ on the basis of 1352 unique data ($F_o^2 > 3\sigma(F_o^2)$). In $[Cu(PMA)]^+$ (**3**), five nitrogen donor centers located in the primary and secondary amines, pyrimidine and imidazole rings, and the amide moiety of PMA^- (the dissociable H is the amide H) are coordinated to copper to give rise to a distorted square-pyramidal geometry. The sixth coordination site on copper is vacant. The spectral properties of $[Cu(PMA)]^+$ (**3**) are remarkably similar to those of Cu(II)-BLM. The crystal structure of $[Cu(PMA)]^+$ in two salts (**3a,b**) confirms the proposed coordination structure of copper in Cu(II)-BLM. Prior to this report, no synthetic analogue of M-BLM had been isolated in the crystalline form. The crystal structure of a second copper complex, namely, $\{[Cu(PMAH)](ClO_4)_2 \cdot H_2O\}_2$ (**4**), which is an intermediate in the reaction path leading to the formation of **3**, has also been determined. Complex **4** crystallizes in the monoclinic space group $P2_1/c$ with $a = 10.956$ (4) Å, $b = 8.907$ (4) Å, $c = 23.252$ (9) Å, $\beta = 93.95$ (3)°, $V = 2264$ (2) Å^3, and $Z = 4$. On the basis of 1633 unique data, the structure of **4** was refined to $R = 5.28\%$. Since **4** is isolated from acidic solutions, the amide group of PMAH remains protonated and does not participate in coordination. In a centrosymmetric dimeric structure, PMAH employs three nitrogens to bind one copper while the imidazole nitrogen is bonded to the other copper center. Additional coordination by one perchlorate ion results in a square-pyramidal geometry around each copper. **3** and **4** are interconvertible. In aqueous solution at neutral pH, **4** is rapidly converted into **3**. Implications of structure(s) like **4** in the process of formation of Cu(II)-BLM have been discussed. In aqueous phosphate buffer (pH 7), **3** is reduced by dithiothreitol to a Cu(I) species that upon oxygenation produces the •OH radical and induces double-strand breaks in DNA.

The metal ion promoted aerobic activation of *bleomycins* (BLMs, **1**) and subsequent strand scission of cellular DNA are two important issues with respect to the antineoplastic activity of this family of glycopeptide antitumor drugs.[1-8] The coordination structures of the metallobleomycins (M-BLMs) lie at the epicenter of the complex chemistry of the drug-DNA interaction. Unfortunately, despite myriad publications,[3-6] precise structural information on M-BLMs is scarce. So far, the coordination structures of M-BLMs have been predicted primarily on the basis of spectroscopic data. The only exception is the proposed structure of Cu(II)-BLM, which is derived from the preliminary crystal structure of the copper(II) complex of P-3A, a putative peptide fragment of BLM.[9] This assignment, however, ignores significant differences between spectral parameters of Cu(II)-BLM and Cu(II)-P-3A. For example, the absorption spectrum, EPR parameters, and half-wave potential of Cu(II)-P-3A are distinctly different from those of Cu(II)-BLM.[10,11] The nature of the mediators of oxidative damage to DNA is also a subject of debate. Earlier, it was proposed that "activated" M-BLMs generate highly reactive oxygen-based free radicals like •OH and $O_2^{\bullet-}$, which inflict strand breaks in cellular DNA.[12] Involvement of freely diffusible active radical species in sequence-specific DNA degradation by Fe-BLM has, however, been questioned.[13] More recent studies indicate that the reactive form of oxygen remains bound to a distinct Fe-BLM complex and induces base release from DNA through 4′-C-H bond cleavage of the deoxyribose sugar moiety.[1] Clearly, structural information on M-BLMs with M in at least two oxidation states is a crucial need in elucidation of the mechanisms of both the free-radical formation and the interaction(s) of the activated M-BLMs with DNA.

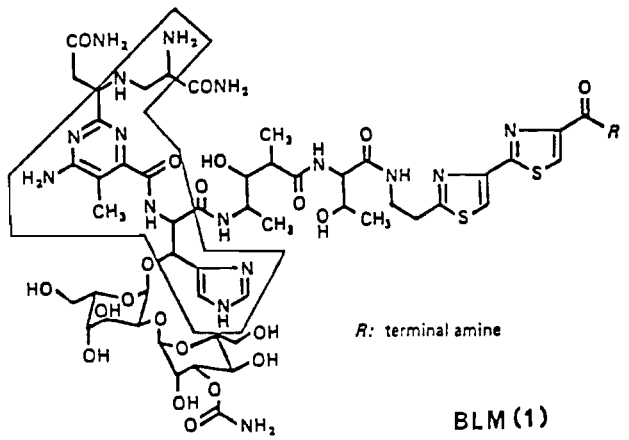

BLM (1)

The scarcity of accurate structural data on M-BLMs is a direct consequence of the usual problems one encounters in crystallization of complex macromolecules. One rational alternative in such a situation is the "synthetic analogue approach",[14] which necessitates (i) syntheses of smaller organic frameworks that show resemblance to or consist of the metal-chelating portion of BLM and (ii) structural studies on the metal complexes of these tailored ligands. Though such an approach has been undertaken by others,[10,11,15-17]

* To whom correspondence should be addressed at the University of California.
† University of Windsor.

(1) Stubbe, J.; Kozarich, J. W. *Chem. Rev.* **1987**, *87*, 1107.
(2) Hecht, S. M. *Acc. Chem. Res.* **1986**, *19*, 383.
(3) Sugiura, Y.; Takita, T.; Umezawa, H. *Met. Ions Biol. Syst.* **1985**, *19*, 81.
(4) Dabrowiak, J. C. *Adv. Inorg. Biochem.* **1983**, *4*, 69.
(5) Povrick, L. F. *Molecular Aspects of Anticancer Drug Action*; Neidle, S., Waring, M. J., Eds.; Macmillan: London, 1983; p 157.
(6) Dabrowiak, J. C. *Met. Ions Biol. Syst.* **1980**, *11*, 305.
(7) Umezawa, H.; Takita, T. *Struct. Bonding (Berlin)* **1980**, *40*, 73.
(8) (a) *Bleomycin: Chemical, Biochemical and Biological Aspects*; Hecht, S. M., Ed.; Springer-Verlag: New York, 1979. (b) *Bleomycin: Current Status and New Developments*; Carter, S. K., Crooke, S. T., Umezawa, H., Eds.; Academic: New York, 1978.
(9) Iitaka, Y.; Nakamura, H.; Nakatani, T.; Muraoka, Y.; Fuji, A.; Takita, T.; Umezawa, H. *J. Antibiot.* **1978**, *31*, 1070.
(10) Umezawa, H.; Takita, T.; Sugiura, Y.; Otsuka, M.; Kobayashi, S.; Ohno, M. *Tetrahearon* **1984**, *40*, 501.
(11) Sugiura, Y.; Suzuki, T.; Otsuka, M.; Kobayashi, S.; Ohno, M.; Takita, T.; Umezawa, H. *J. Biol. Chem.* **1983**, *258*, 1328.
(12) Burger, R. M.; Peisach, J.; Blumberg, W. E.; Horwitz, S. B. *J. Biol. Chem.* **1979**, *254*, 10906.
(13) Rodriguez, L. O.; Hecth, S. M. *Biochem. Biophys. Res. Commun.* **1982**, *104*, 1470.
(14) Ibers, J. A.; Holm, R. H. *Science (Washington, D.C.)* **1980**, *209*, 223.
(15) (a) Kittaka, A.; Sugano, Y.; Otsuka, M.; Ohno, M. *Tetrahedron* **1988**, *44*, 2811, 2821. (b) Kittaka, A.; Sugano, Y.; Otsuka, M.; Ohno, M.; Sugiura, Y.; Umezawa, H. *Tetrahedron Lett.* **1986**, *27*, 3631, 3635. (c) Otsuka, M.; Yoshida, M.; Kobayashi, S.; Ohno, M.; Sugiura, Y.; Takita, T.; Umezawa, H. *J. Am. Chem. Soc.* **1981**, *103*, 6986.

0020-1669/89/1328-0468$01.50/0

attempts so far have only been restricted to studies on the metalated analogues in solution. Not surprisingly, uncertainties related to the structures of the metal-containing species in solution persisted in such attempts. For example, in the most recent report,[15b] at least four different structures have been proposed as the possible structure for the iron analogue. The need for crystallographic studies on the synthetic analogues thus remains crucial.

In our systematic synthetic analogue approach to M–BLMs, we have been involved in *structural* and spectroscopic characterization of metal complexes of organic fragments that mimic part of the metal-chelating section of BLM.[18-21] Apart from important structural data pertinent to the proposed structures of M–BLMs, our work has reemphasized the risk associated with structure assignment on the basis of spectroscopic data alone. In order to avoid ambiguity, we have restricted our attempts to isolation and characterization of *crystalline* synthetic analogues. Very recently,[22] we have reported the synthesis of a tailored ligand PMAH (**2**),[23] which mimics a major part of the metal-chelating

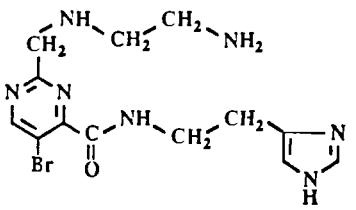

PMAH
(**2**)

locus of BLM (boxed area in **1**). This ligand contains five nitrogen donor centers located in the primary and secondary amines, pyrimidine and imidazole rings, and the amide moiety. A brief description of the structure of the copper(II) complex of this designed ligand, namely, $[Cu(PMA)]BF_4$ (**3a**), is also included in our previous communication. It is important to note that PMAH is the first synthetic analogue of BLM that is based on a pyrimidine ring. All the other reported analogues[10,11,15-17] contain (unlike BLM) a pyridine ring in their organic frameworks. Here, we provide a complete report on the structure of $[Cu(PMA)]ClO_4 \cdot 0.5H_2O \cdot 0.5CH_3OH$ (**3b**). $[Cu(PMA)]^+$ is the first synthetic analogue of Cu(II)–BLM (or any M–BLM) characterized structurally in the crystalline state. Extensive spectroscopic correlation and comparison between $[Cu(PMA)]^+$ and Cu(II)–BLM are also included.

During the past few years, several reports describing various pH-dependent modes of BLM ligation to copper have appeared.[24,25] Following successful characterization of $[Cu(PMA)]X$ ($X = BF_4$, ClO_4), we became interested in this aspect of BLM chemistry. Herein, we report that small variation in pH (~3 units) allows PMAH to bind copper(II) in two strikingly different ways. Detailed in this report are the synthesis, spectral properties, and structure of a second copper(II) complex $\{[Cu(PMAH)](ClO_4)_2 \cdot H_2O\}_2$ (**4**), in which ligation of PMAH to copper is very different from that observed in **3b** (or **3a**). The two structures **4** and **3b** are interconvertible. The implications of these two structures in solutions of Cu(II)–BLM at different pHs are also discussed.

Experimental Section

Preparation of Compounds. Mucobromic acid, histamine (free base), thionyl chloride, lithium perchlorate, and copper(II) acetate monohydrate were procured from Aldrich Chemical Co. and were used without further purification. Ethylenediamine (Aldrich) was distilled before use. Hydroxyacetonitrile (50% aqueous solution) was purchased from CTC Organics, Atlanta, GA. The key intermediate, 2-(hydroxymethyl)-5-bromo-4-pyrimidinecarboxylic acid was synthesized by following the literature procedure.[26] The synthesis and spectral parameters of PMAH have already been reported by us in a previous communication.[22]

$[Cu(PMA)]BF_4$ (3a). A solution of 220 mg (0.6 mmol) of PMAH in 5 mL of methanol was slowly added with stirring to a solution of 100 mg (0.5 mmol) of copper(II) acetate monohydrate in 30 mL of methanol, and the resultant turquoise solution was stirred for 3 h at room temperature. A batch of 57 mg (0.6 mmol) of $LiBF_4$ in 4 mL of methanol was then added, and the mixture was filtered to remove any suspended particles. The clear greenish blue filtrate was kept at room temperature to allow slow evaporation. Deep greenish blue blocks were deposited within 24 h. The crystals were collected by filtration, washed with cold methanol, and dried in air; yield 130 mg (50%). Anal. Calcd for $CuC_{13}H_{17}N_7OBrBF_4$: C, 30.15; H, 3.31; N, 18.95. Found: C, 30.62; H, 3.21; N, 18.75. Selected IR bands (KBr pellet, cm^{-1}): 3360 (s), 3120 (s), 3040 (m), 2920 (s), 1600 (vs, ν_{CO}), 1560 (s), 1520 (w), 1460 (m), 1400 (w), 1360 (m), 1280 (w), 1240 (w), 1080 (vs, br, BF_4^-), 950 (m), 840 (br, m), 805 (w), 710 (m), 690 (m), 650 (w), 640 (w), 550 (w), 530 (w). Value of μ_{eff}(298 K, polycryst): 1.72 μ_B.

$[Cu(PMA)]ClO_4 \cdot 0.5H_2O \cdot 0.5CH_3OH$ (3b). The turquoise solution that resulted from mixing 121 mg (0.33 mmol) of PMAH and 55 mg (0.28 mmol) of copper(II) acetate monohydrate in 20 mL of methanol was stirred for 3 h at room temperature. Next, a batch of 35 mg (0.33 mmol) of $LiClO_4$ in 15 mL of methanol was added and the slightly cloudy mixture was filtered. The greenish blue filtrate, on slow evaporation, afforded 80 mg (54%) of deep greenish blue blocks, which were collected by filtration, washed with methanol, and dried in air. Anal. Calcd for $CuC_{13.5}H_{20}N_7O_6ClBr$: C, 29.18; H, 3.63; N, 17.66. Found: C, 28.87; H, 3.51; N, 17.65. The IR spectrum of **3b** is identical with that of **3a** except for ClO_4^- vibrations (1120 cm^{-1} (vs, br); 630 cm^{-1} (s)). Value of μ_{eff}(298 K, polycryst): 1.74 μ_B.

$\{[Cu(PMAH)](ClO_4)_2 \cdot H_2O\}_2$ (4). A solution of 132 mg (0.36 mmol) of PMAH in 5 mL of methanol was slowly added with constant stirring to a methanolic solution (10 mL) of copper(II) perchlorate hexahydrate (110 mg, 0.30 mmol). Along with the addition of the ligand was also added, in small aliquots, a total of 2.5 mL of water to dissolve the blue precipitate formed during this period. Next, a batch of 63 mg (0.6 mmol) of $LiClO_4$ dissolved in 5 mL of methanol was added to this mixture. Finally, 2 mL of water was used to remove turbidity and the mixture was filtered to eliminate trace amounts of flocculent precipitate. The clear blue filtrate was stored over concentrated H_2SO_4 under vacuum. A batch of 80 mg (42%) of bluish purple blocks was obtained after 48 h. Anal. Calcd for $CuC_{13}H_{20}N_7O_{10}Cl_2Br$: C, 24.05; H, 3.11; N, 15.12. Found: C, 24.10; H, 3.28; N, 15.32. Selected IR bands (KBr pellet, cm^{-1}): 3240 (vs, br), 1660 (vs, ν_{CO}), 1600 (m), 1570 (s), 1540 (m), 1440 (s), 1340 (m), 1300 (w), 1120 (vs, br, ClO_4^-), 850 (m), 820 (w), 660 (s), 630 (s, ClO_4^-). Value of μ_{eff}(298 K, polycryst): 1.79 μ_B/Cu atom.

Conversion of 3b into 4. A batch of 66 mg (0.125 mmol) of **3b** was dissolved in a mixture of 10 mL of water and 3 mL of methanol, and the pH was adjusted to 4 with $HClO_4$.[27] The initial turquoise color changed into a clear blue. After the addition of a solution of 53 mg (0.5 mmol) of $LiClO_4$ in 1 mL of water the mixture was filtered to remove any suspended particle. The blue filtrate on storage over concentrated H_2SO_4 afforded 40 mg (50%) of **4** as purple needles. The identity of the product was confirmed by IR and electronic absorption spectroscopy.

Conversion of 4 into 3b. A clear blue solution of **4** was prepared from 132 mg (0.36 mmol) of PMAH and 110 mg (0.3 mmol) of copper(II) perchlorate hexahydrate by following the procedure described above. It was then divided into two equal parts (12.5 mL each). To part I, a batch of 31 mg (0.38 mmol) of sodium acetate in 1 mL of methanol was added when a color change of blue to turquoise was observed. The turquoise solution, on evaporation in air, afforded 40 mg (~50%) of **3b** as greenish blue blocks. Part II, on the other hand, was stored over concentrated

(16) Kurosaki, H.; Anan, H.; Kimura, E. *J. Chem. Soc. Jpn.* **1988**, *4*, 691.
(17) (a) Kenani, A.; Lohez, M.; Houssin, R.; Helbecque, N.; Bernier, J.-L.; Lemay, P.; Henichart, J.-P. *Anti-Cancer Drug Des.* **1987**, *2*, 47. (b) Henichart, J.-P.; Bernier, J.-L.; Houssin, R.; Lohez, M.; Kenani, A.; Catteau, J.-P. *Biochem. Biophys. Res. Commun.* **1985**, *126*, 1036. (c) Henichart, J.-P.; Houssin, R.; Bernier, J.-L.; Catteau, J.-P. *J. Chem. Soc., Chem. Commun.* **1982**, 1295.
(18) Brown, S. J.; Tao, X.; Stephan, D. W.; Mascharak, P. K. *Inorg. Chem.* **1986**, *25*, 3377.
(19) Tao, X.; Stephan, D. W.; Mascharak, P. K. *Inorg. Chem.* **1987**, *26*, 754.
(20) Delany, K.; Arora, S. K.; Mascharak, P. K. *Inorg. Chem.* **1988**, *27*, 705.
(21) Brown, S. J.; Tao, X.; Wark, T. A.; Stephan, D. W.; Mascharak, P. K. *Inorg. Chem.* **1988**, *27*, 1581.
(22) Brown, S. J.; Stephan, D. W.; Mascharak, P. K. *J. Am. Chem. Soc.* **1988**, *110*, 1996.
(23) The dissociable H is the amide H.
(24) Bereman, R. D.; Winkler, M. E. *J. Inorg. Biochem.* **1980**, *13*, 95.
(25) (a) Solaiman, D.; Rao, E. A.; Antholine, W.; Petering, D. H. *J. Inorg. Biochem.* **1980**, *12*, 201. (b) Albertini, J.-P.; Suillerot, A. G. *J. Inorg. Biochem.* **1985**, *25*, 15.
(26) Kim, D. H.; McKee, R. L. *J. Org. Chem.* **1970**, *35*, 455.
(27) An Orion Research Model 601A pH meter was used to monitor the apparent pH values (solution contained ~25% methanol).

Table I. Summary of Crystal Data, Intensity Collection, and Structure Refinement Parameters for $[Cu(PMA)]ClO_4 \cdot 0.5H_2O \cdot 0.5CH_3OH$ (**3b**) and $\{[Cu(PMAH)](ClO_4)_2 \cdot H_2O\}_2$ (**4**)

	3b	**4**
formula (mol wt)	$CuC_{13.5}H_{20}N_7O_6ClBr$ (555.09)	$CuC_{13}H_{20}N_7O_{10}Cl_2Br$ (648.56)
cryst color, form	dark greenish blue blocks	deep blue blocks
a, Å	14.934 (6)	10.956 (4)
b, Å	15.617 (8)	8.907 (4)
c, Å	17.856 (8)	23.252 (9)
β, deg		93.95 (3)
cryst syst	orthorhombic	monoclinic
space group	*Pbca*	$P2_1/c$
V, Å^3	4164 (3)	2264 (2)
d_{calcd}, g/cm^3	1.77	1.90
d_{obsd},[a] g/cm^3	1.76 (2)	1.89 (2)
Z	8	4
cryst dimens, mm	0.35 × 0.35 × 0.27	0.38 × 0.38 × 0.42
abs coeff (μ), cm^{-1}	30.37	28.15
radiation (λ, Å)	Mo Kα (0.71069)	Mo Kα (0.71069)
temp, °C	24	24
scan speed, deg/min	2.0–5.0 ($\theta/2\theta$ scan)	2.0–5.0 ($\theta/2\theta$ scan)
scan range, deg	1.0 below Kα_1 to 1.0 above Kα_2	1.0 below Kα_1 to 1.0 above Kα_2
bdgd/scan time ratio	0.5	0.5
no. of data collcd	3098	3213
no. of unique data ($F_o^2 > 3\sigma(F_o^2)$)	1352	1633
no. of variables	200	242
R, %	5.84	5.28
R_w, %	6.22	5.67
max Δ/σ in final least-squares cycle	0.002	0.007
largest resid electron dens, e/Å^3	0.97	0.63
atom(s) associated with resid dens	C20, O20	C12

[a] Determined by flotation in $CCl_4/CHBr_3$.

H_2SO_4, and after 60 h, blue crystals of **4** were obtained in ~40% yield. The latter procedure demonstrated that indeed we have **4** in the initial blue solution.

Observations were practically identical when $Cu(BF_4)_2$ was used as the source of copper in the experiment described above. Crystals of **3a** were isolated in good yields from such attempts.

X-ray Data Collection and Reduction. Crystals of **3b** and **4** were obtained by slow evaporation of solutions of the complexes in aqueous methanol. Diffraction experiments were performed on a four-circle Syntex $P2_1$ diffractometer with graphite-monochromatized Mo Kα radiation. The initial orientation matrices were obtained from 15 machine-centered reflections selected from rotation photographs. These data were used to determine the crystal systems. Partial rotation photographs around each axis were consistent with orthorhombic and monoclinic crystal systems for **3b** and **4**, respectively. Ultimately, 30 and 64 high-angle reflections ($20° < 2\theta < 25°$) were used to obtain the final lattice parameters and the orientation matrices for **3b** and **4**, respectively. The observed extinctions were consistent with the space group *Pbca* for **3b** and $P2_1/c$ for **4**. During data collection ($4.5° < 2\theta < 45°$: for **3b**, $+h,+k,+l$ data; for **4**, $\pm h,+k,+l$ data), intensities of three check reflections were monitored after every 197 reflections. Their intensities showed no statistically significant change over the duration of data collection. The data were processed by using the SHELX-76 program package.[28] An empirical absorption correction was applied to each data set on the basis of refinement of three ψ scans. Machine parameters, crystal data, and data collection parameters are summarized in Table I.

Structure Solution and Refinement. Non-hydrogen atomic scattering factors were taken from literature tabulations.[29] Positions for the Br and the Cu atom were determined by direct methods in both cases. The remaining non-hydrogen atoms were located from successive difference Fourier map calculations. Refinements were carried out by using full-matrix least-squares techniques on F, minimizing the function $\sum w(|F_o| - |F_c|)^2$, where the weight w is defined as $4F_o^2/\sigma^2(F_o^2)$ and F_o and F_c are the observed and calculated structure factor amplitudes. The Cu, Br, N, Cl, and O atoms were refined with anisotropic thermal parameters. The remaining atoms were assigned isotropic temperature factors. Hydrogen atom positions were calculated and allowed to ride on the carbon or nitrogen atoms to which they are bonded; the C–H and the N–H bond lengths were assumed to be 0.95 and 1.01 Å, respectively. Temperature factors for the hydrogen atoms were fixed at 1.10 times the isotropic temperature factor of the carbon atom to which the hydrogen is bonded. In case of **3b**, fractional occupancy and disorder of the solvent molecules precluded location of the hydrogen atoms associated with them. In all cases, the hydrogen atom contributions were calculated but not refined. In both structures, slight disorder of the perchlorate group(s) is reflected in the large thermal parameters for the oxygen atoms as well as in small deviations from the ideal geometry. No attempts were made to model these disorders. The final values of $R = \sum||F_o| - |F_c||/\sum|F_o|$ and $R_w = [\sum w(|F_o| - |F_c|)^2/\sum w(F_o^2)]^{1/2}$ are given in Table I. The maximum Δ/σ value on any of the parameters in the final cycle of refinement for each compound is also included in Table I. The residual electron densities were of no chemical significance. The following data are tabulated: positional parameters (Table II) and selected bond distances and angles (Table III). Thermal parameters (Table S1), hydrogen atom parameters (Table S2), bond distances and angles associated with the perchlorate groups (Table S3), and values of $10|F_o|$ and $10|F_c|$ (Table S4) have been deposited as supplementary material.

Other Physical Measurements. Elemental analyses were performed by Atlantic Microlabs Inc., Atlanta, GA. Infrared spectra were measured with a Nicolet MX-S FT spectrophotometer. Absorption spectra were recorded on a Perkin-Elmer Lambda 9 spectrophotometer. EPR spectra were obtained at X-band frequencies by using a Varian E-3 spectrometer connected to a Digital PDP 11 computer for data manipulation. A Johnson Matthey magnetic susceptibility balance was used to monitor the room-temperature susceptibility values in the polycrystalline state. Diamagnetic corrections were calculated from Pascal constants.[30] Electrochemical measurements were completed with standard Princeton Applied Research instrumentation using a Model 303 static mercury-drop electrode; potentials were measured at ~25 °C vs an Ag/AgCl electrode as reference. The spin-trapping experiments were performed by using 5,5-dimethyl-1-pyrroline *N*-oxide (DMPO, Aldrich Chemical Co.) as the spin trap. Experimental conditions: concentration of the trap, 100 mM; 10 mM phosphate buffer (pH 7.5); concentration of **3**, 1 mM; concentration of dithiothreitol (DTT, reductant), 1 mM; oxygen bubbled for 60 s at 20 °C; aqueous flat cell used to record ESR spectra of the spin adducts.

DNA Cleavage Experiments. Reaction mixtures (10-μL total volume) contained 1 μg of DNA (pBR322 or ϕX174 (rf)) in 3 mM phosphate buffer (pH 7.4), 10^{-4}–10^{-6} M **3**, and 5×10^{-4} M DTT. Nanopure water was used. Following incubation at 37 °C for 1 h, the reactions were quenched with 2 μL of 0.5 M EDTA and the DNA was immediatelly precipitated with cold ethanol. The DNA pellets were then dissolved in 10 mM Tris-HCl buffer (pH 8) containing 1 mM EDTA, and ~0.2-μg

(28) Sheldrick, G. M. "SHELX-76 Program for Crystal Structure Determination"; University of Cambridge: Cambridge, England, 1976.
(29) *International Tables for X-ray Crystallography*; Kynoch: Birmingham, England, 1974; Vol. IV.
(30) Mulay, L. N. In *Physical Methods of Chemistry*; Weissberger, A., Rossiter, B. W., Eds.; Wiley-Interscience: New York, 1972; Part IV, Chapter VII.

Table II. Positional Parameters[a]

atom	x	y	z	atom	x	y	z
			Molecule **3b**				
Br	4645 (1)	5447 (1)	6864 (1)	Cu	3518 (1)	3657 (1)	4245 (1)
Cl	1464 (4)	−245 (4)	1432 (3)	O1	4815 (6)	3602 (6)	6238 (5)
O11	1467 (15)	339 (12)	1995 (8)	O12	1742 (14)	82 (12)	795 (7)
O13	600 (13)	−491 (13)	1423 (15)	O14	1995 (13)	−940 (12)	1595 (14)
O20	1625 (16)	2005 (16)	1252 (14)	N1	3827 (8)	2717 (7)	3590 (6)
N2	4342 (8)	1887 (8)	2680 (5)	N3	4207 (7)	3232 (7)	5110 (5)
N4	3416 (7)	6189 (7)	4924 (6)	N5	3668 (7)	4721 (7)	4820 (5)
N6	2894 (7)	4540 (8)	3506 (5)	N7	2114 (8)	3300 (6)	4521 (4)
C1	3982 (10)	2656 (11)	2870 (9)	C2	4426 (10)	1424 (11)	3322 (8)
C3	4134 (9)	1929 (9)	3891 (7)	C4	4017 (11)	1731 (10)	4703 (8)
C5	4528 (10)	2336 (9)	5198 (8)	C6	4388 (8)	3765 (8)	5658 (8)
C7	4067 (8)	4664 (8)	5490 (7)	C8	4135 (8)	5385 (9)	5907 (7)
C9	3788 (9)	6128 (9)	5593 (8)	C10	3374 (8)	5455 (10)	4562 (7)
C11	3037 (10)	5418 (10)	3772 (8)	C12	1991 (14)	4304 (14)	3441 (12)
C13	1622 (16)	4013 (15)	4078 (12)	C20	2517 (21)	2132 (28)	1662 (22)
			Molecule **4**				
Br	1776 (1)	9033 (1)	0241 (0)	Cu	−1998 (1)	6342 (2)	−1363 (1)
Cl1	301 (3)	3543 (4)	−1132 (1)	Cl2	2981 (4)	5348 (5)	−3029 (2)
O1	3953 (7)	8714 (8)	−960 (5)	O2	−3954 (8)	14276 (9)	1302 (4)
O11	−906 (10)	3869 (13)	−1320 (7)	O12	1110 (11)	4311 (15)	−1435 (7)
O13	260 (16)	4132 (17)	−564 (6)	O14	584 (11)	2112 (13)	−1048 (8)
O21	2068 (24)	5453 (21)	−2725 (13)	O22	3397 (14)	6642 (15)	−3234 (9)
O23	3892 (22)	4508 (30)	−2747 (12)	O24	2771 (23)	4310 (20)	−3430 (7)
N1	−3345 (8)	5605 (10)	216 (4)	N2	−2723 (7)	6276 (10)	−620 (3)
N3	−3064 (7)	9018 (9)	971 (3)	N4	−425 (7)	7434 (9)	−1118 (3)
N5	1354 (7)	8387 (10)	−1514 (3)	N6	−1345 (11)	6547 (16)	−2124 (4)
N7	−3384 (8)	5255 (13)	−1800 (4)	C1	−2626 (11)	5269 (14)	−220 (5)
C2	−3563 (9)	7300 (12)	−447 (4)	C3	−3955 (9)	6933 (11)	69 (4)
C4	−4782 (10)	7685 (13)	460 (5)	C5	−4159 (9)	8137 (12)	1031 (4)
C6	−3055 (9)	10502 (11)	961 (4)	C7	1798 (9)	8773 (10)	−979 (4)
C8	1132 (9)	8533 (11)	−506 (4)	C9	34 (8)	7812 (10)	−595 (4)
C10	260 (9)	7736 (11)	−1556 (4)	C11	−242 (10)	7288 (13)	−2142 (5)
C12	−2096 (13)	6008 (17)	−2551 (6)	C13	−3204 (15)	5243 (18)	−2418 (7)

[a] Multiplied by 10^4.

portions of DNA (plus 5 μL of loading dye) were loaded onto 1% agarose gels. Horizontal gel electrophoresis was carried out at 100 V for 3 h. The gels were stained with ethidium and photographed under UV light. A Hoefer Scientific Instruments scanning densitometer (Model GS 300) was used to determine the amounts of the DNA cleavage products on the gels.

Results and Discussion

Structure of $[Cu(PMA)]ClO_4 \cdot 0.5H_2O \cdot 0.5CH_3OH$ (3b). A preliminary report on the structure of $[Cu(PMA)]BF_4$ (**3a**) was communicated earlier.[22] Unfortunately, due to the poor quality of the crystals of **3a** in general,[31] a satisfactory number of unique reflections were not obtained in two different attempts. Structure determination of $[Cu(PMA)]^+$ has therefore been completed with the use of the perchlorate salt. It must be emphasized here that the reported structure of $[Cu(PMA)]^+$ in **3a** is practically identical with that observed in **3b**. The present structure is, however, more precise as compared to the one reported earlier.

Crystals of **3b** are made up of unit cells each containing eight $[Cu(PMA)]^+$ ions and an equivalent number of ClO_4^- ions. An ORTEP drawing of the cation is shown in Figure 1, and selected interatomic distances and angles are listed in Table III. The closest approach of the cation to the anion is 2.280 Å (O11···HN6). Hydrogen bonding between the lattice methanol and the perchlorate anion is suggested by the O20···O11 distance (2.930 Å), while the water molecule appears to be hydrogen bonded to HN7 (OW···HN7 = 2.341 Å).

The coordination geometry of copper in $[Cu(PMA)]^+$ is distorted square pyramidal. Four nitrogens from the imidazole (N1), pyrimidine (N5), secondary amine (N6), and the deprotonated amide group (N3) form the basal plane of coordination while the primary amine nitrogen (N7) occupies the axial position. The ligand is thus pentadentate and anionic. The copper atom is displaced 0.24 (1) Å from the mean basal plane in the direction

(31) Large crystals of **3a** can be grown. However, the crystals often diffract rather poorly.

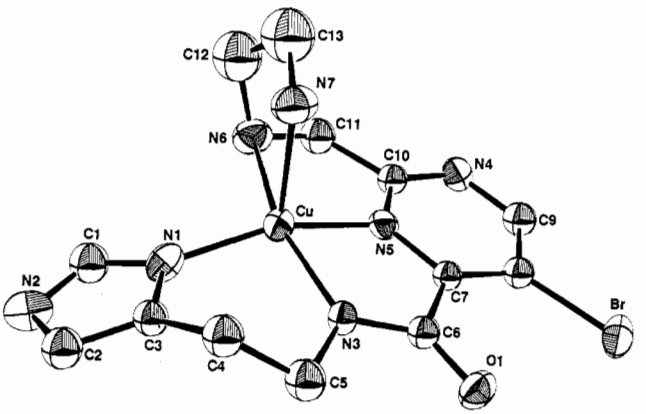

Figure 1. ORTEP drawing of $[Cu(PMA)]^+$ in **3b**, showing 30% probability ellipsoids and the atom-labeling scheme. Hydrogen atoms and the lattice solvent molecules (partial occupancy) are omitted for clarity.

of N7. It is interesting to note that the mode of binding and the orientation of part of the ligand containing the N1, N3, and N5 donor centers (Figure 1) are distinctly reminiscent of those of PmpepH (**5**) in $[Cu(Pmpep)(CH_3COO)(H_2O)]$.[18] In fact, cor-

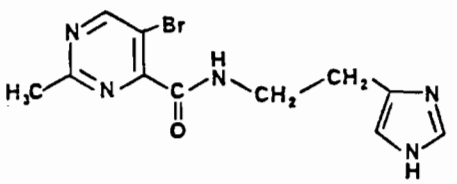

PmpepH (5)

responding bond distances and angles are quite comparable in $[Cu(PMA)]^+$ and $[Cu(Pmpep)(CH_3COO)(H_2O)]$. For example, the Cu–N(imidazole) bond is 1.93 (1) and 1.960 (5) Å long in

Table III. Selected Bond Distances and Angles

Molecule **3b**

Distances (Å)

Cu–N1	1.93 (1)	Cu–N3	1.97 (1)	Cu–N5	1.97 (1)
Cu–N6	2.13 (1)	Cu–N7	2.23 (1)	C1–N1	1.31 (2)
C3–N1	1.42 (2)	C1–N2	1.36 (2)	C2–N2	1.36 (2)
C5–N3	1.49 (2)	C6–N3	1.31 (2)	C9–N4	1.32 (2)
C10–N4	1.32 (2)	C7–N5	1.34 (1)	C10–N5	1.31 (2)
C11–N6	1.47 (2)	C12–N6	1.40 (2)	C13–N7	1.55 (2)
C2–C3	1.36 (2)	C3–C4	1.49 (2)	C4–C5	1.50 (2)
O1–C6	1.24 (2)	C6–C7	1.51 (2)	C7–C8	1.35 (2)
C8–C9	1.39 (2)	C10–C11	1.50 (2)	C12–C13	1.34 (2)

Angles (deg)

N3–Cu–N1	95.4 (4)	N5–Cu–N1	158.6 (5)
N5–Cu–N3	79.4 (4)	N6–Cu–N1	102.8 (4)
N6–Cu–N3	159.1 (5)	N6–Cu–N5	79.9 (4)
N7–Cu–N1	99.7 (4)	N7–Cu–N3	103.6 (4)
N7–Cu–N5	101.7 (4)	N7–Cu–N6	83.5 (4)
C1–N1–Cu	134 (1)	C3–N1–Cu	120.4 (8)
C3–N1–C1	105 (1)	C2–N2–C1	107 (1)
C5–N3–Cu	124.6 (9)	C6–N3–Cu	118.6 (9)
C6–N3–C5	117 (1)	C10–N4–C9	114 (1)
C7–N5–Cu	117.4 (9)	C10–N5–Cu	121.2 (8)
C10–N5–C7	121 (1)	C11–N6–Cu	110 (8)
C12–N6–Cu	108 (1)	C12–N6–C11	114 (1)
C13–N7–Cu	99 (1)	N2–C1–N1	113 (1)
C3–C2–N2	107 (1)	C2–C3–N1	109 (1)
C4–C3–N1	121 (1)	C4–C3–C2	130 (1)
C5–C4–C3	112 (1)	C4–C5–N3	112 (1)
N3–C6–O1	127 (1)	C7–C6–O1	121 (1)
C7–C6–N3	112 (1)	C6–C7–N5	112 (1)
C8–C7–N5	118 (1)	C8–C7–C6	130 (1)
C9–C8–C7	117 (1)	C8–C9–N4	126 (1)
N5–C10–N4	125 (1)	C11–C10–N4	121 (1)
C11–C10–N5	114 (1)	C10–C11–N6	113 (1)
C13–C12–N6	114 (2)	C12–C13–N7	119 (2)

Molecule **4**

Distances (Å)

Cu–O11	2.51 (1)	Cu–N2	1.951 (8)	Cu–N4	2.026 (7)
Cu–N6	1.96 (1)	Cu–N7	2.016 (9)	C1–N1	1.36 (1)
C3–N1	1.39 (1)	C1–N2	1.29 (1)	C2–N2	1.38 (1)
C5–N3	1.45 (1)	C6–N3	1.32 (1)	Cu–N4	2.026 (7)
C9–N4	1.33 (1)	C10–N4	1.34 (1)	C7–N5	1.35 (1)
C10–N5	1.33 (1)	C11–N6	1.38 (1)	C12–N6	1.33 (2)
C13–N7	1.47 (2)	C2–C3	1.34 (1)	C3–C4	1.49 (1)
C4–C5	1.51 (1)	C7–C8	1.38 (1)	C8–C9	1.37 (1)
C10–C11	1.49 (2)	C12–C13	1.44 (2)		

Angles (deg)

N2–Cu–O11	99.2 (5)	N4–Cu–O11	90.9 (3)
N4–Cu–N2	98.9 (3)	N6–Cu–O11	85.1 (6)
N6–Cu–N2	175.6 (5)	N6–Cu–N4	81.6 (3)
N7–Cu–O11	86.5 (4)	N7–Cu–N2	95.4 (4)
N7–Cu–N4	165.7 (4)	N7–Cu–N6	84.2 (4)
Cl1–O11–Cu	129.5 (7)	C3–N1–C1	107.3 (9)
C1–N2–Cu	129.8 (8)	C2–N2–Cu	124.1 (7)
C2–N2–C1	105.9 (9)	C6–N3–C5	123.5 (9)
C9–N4–Cu	129.9 (6)	C10–N4–Cu	113.2 (6)
C10–N4–C9	116.8 (8)	C10–N5–C7	116.5 (8)
C11–N6–Cu	116.5 (7)	C12–N6–Cu	113.2 (9)
C12–N6–C11	130 (1)	C13–N7–Cu	110.5 (8)
N2–C1–N1	111 (1)	C3–C2–N2	111.2 (9)
C2–C3–N1	104.4 (9)	C4–C3–N1	122.4 (9)
C4–C3–C2	133 (1)	C5–C4–C3	113.7 (9)
C4–C5–N3	112.9 (9)	C8–C7–N5	121.3 (9)
C9–C8–C7	117.5 (9)	C8–C9–N4	122.2 (9)
N5–C10–N4	125.7 (9)	C11–C10–N4	116.9 (9)
C11–C10–N5	117.4 (9)	C10–C11–N6	112 (1)

[Cu(PMA)]$^+$ and [Cu(Pmpep)(CH_3COO)(H_2O)], respectively.[32] The reported Cu–N(pyrimidine) distances lie in the narrow range 1.95–2.05 Å.[33] In [Cu(PMA)]$^+$ (Table III), the Cu–N(pyrimidine) bond is 1.97 (1) Å long. The Cu–N(peptide) distance (1.97 (1) Å) in [Cu(PMA)]$^+$ is also typical of similar peptide complexes of bivalent copper.[34] In [Cu(dien)$_2$](NO_3)$_2$,[35] the average Cu–N(primary amine) and Cu–N(secondary amine) distances are 2.21 and 2.01 Å, respectively. The Cu–N7 distance (2.23 (1) Å) in [Cu(PMA)]$^+$ thus appears to be normal. In contrast, the Cu–N6 bond (2.13 (1) Å) is somewhat longer presumably due to strain in the five-membered chelate rings.[36] Formation of three five-membered chelate rings also results in significant deviations from 90° for the N–Cu–N angles in [Cu(PMA)]$^+$ (Table III).

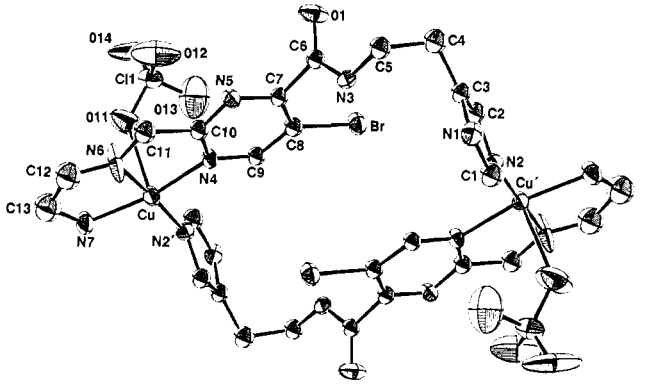

Figure 2. ORTEP drawing of **4**, showing 30% probability ellipsoids and the atom-labeling scheme. The second perchlorate anion, the lattice water molecule, and the hydrogen atoms are all omitted for clarity.

A vacant sixth coordination site on copper is found in both **3a**[22] and **3b**. It is quite probable that the sixth site is less accessible due to steric hindrance from the ligand framework. As will be seen in a later section, the metal center in [Cu(PMA)]$^+$ also remains pentacoordinated in solution.

Structure of {[Cu(PMAH)](ClO_4)$_2$·H_2O}$_2$ (4). Crystals of **4** contain four [Cu(PMAH)](ClO_4)$_2$·H_2O "halves" in the unit cell. The copper-containing fragments pair up to result in centrosymmetric dimers. An ORTEP drawing of the dimer is displayed in Figure 2, and selected bond distances and angles are collected in Table III. The most interesting feature of the dimeric structure is the presence of the ligand in the protonated form (PMAH vs PMA$^-$ in **3a** or **3b**). The geometry around each copper is essentially square pyramidal. Within a dimer (Figure 2), the donors in the basal plane of each copper consist of three nitrogens (N4, N6, N7) from one PMAH and the imidazole nitrogen N2 of the other ligand. The peptide nitrogen remains protonated and does not take part in coordination. An oxygen atom of one of the perchlorate ions occupies the axial position on each copper. The second perchlorate ion is not coordinated. The water molecule is hydrogen bonded to HN1 (O_2···HN1 = 1.928 (4) Å). The Cu–Cu distance within each individual dimer is 7.824 Å, and the closest approach between dimers is 2.448 Å (H_b12···N5).

Inspection of Figures 1 and 2 reveals that the mode of coordination of PMAH to copper in **4** is strikingly different from that observed in [Cu(PMA)]$^+$. Discussions pertinent to this aspect of PMAH chemistry are included in a later section. Only the structural characteristics of **4** are discussed here. The Cu–N7 distance (2.016 (9) Å) in **4** is noticeably shorter than the same distance in **3b** (2.23 (1) Å) as a consequence of the Jahn–Teller effect. The Cu–N6 bond length (1.96 (1) Å), however, compares well with the Cu–N(secondary amine) distance (1.98 (1) Å) reported for a structurally related Me_4dien complex of copper.[37]

(32) Clearly, structures (and spectral properties) of the smaller and simpler synthetic analogues reported by us[18] proved helpful in the present study.
(33) Szalda, D. J.; Marzilli, L. G.; Kistenmacher, T. J. *Biochem. Biophys. Res. Commun.* **1975**, *63*, 601.
(34) (a) Osterberg, R.; Sjoberg, B. *J. Chem. Soc., Chem. Commun.* **1972**, 983. (b) Osterberg, R.; Sjoberg, B.; Soderquist, R. *Acta Chem. Scand.* **1972**, *26*, 4184. (c) Blount, J. F.; Fraser, K. A.; Freeman, H. C.; Szymanski, J. T.; Wang, C.-H. *Acta Crystallogr.* **1967**, *22*, 396. (d) Meester, P. D.; Hodgson, D. J. *Acta Crystallogr.* **1977**, *B33*, 3505.
(35) Stephens, F. S. *J. Chem. Soc. A* **1969**, 883.
(36) N6 is shared by two five-membered chelate rings that are at ~90° to each other.
(37) O'Young, C.-L.; Dewan, J. C.; Lilienthal, H. R.; Lippard, S. J. *J. Am. Chem. Soc.* **1978**, *100*, 7291.

Also, the Cu–N4 (2.026 (7) Å) and Cu–N2 (1.951 (8) Å) distances fall within the normal range of Cu–N(pyrimidine)[33] and Cu–N(imidazole)[34] bond lengths. Relatively weak axial interaction[38] is indicated by the long Cu–O(perchlorate) distance of 2.51 (1) Å. Deviations from 90° are also recorded for the N–Cu–N angles in **4** due to formation of five-membered chelate rings.

The pyrimidine ring in PMAH employs two different nitrogen donor centers to bind copper in $[Cu(PMA)]^+$ and **4** (N5 and N4, respectively). So is the case with the imidazole ring. It has been strongly argued that, of the two nitrogens in the imidazole ring, coordination of a single metal ion occurs at the pyridine rather than the pyrrole-type nitrogen.[39] Since the two nitrogen centers of the imidazole group in PMAH undergo rapid tautomeric exchange in solution,[39] ligation by the pyridine-type nitrogen results in a different connectivity, namely Cu–N2 in **4** as opposed to Cu–N1 in $[Cu(PMA)]^+$.

Syntheses and Interconversions. Since PMAH precisely duplicates a major portion of the metal-chelating locus of BLM, spectral and structural characteristics of the metal complexes of this designed ligand are expected to mimic those of the corresponding M–BLMs very closely. In the present work, two copper(II) complexes of PMAH have been isolated. Reaction of copper(II) acetate with PMAH (ratio 1:1) in methanol affords $[Cu(PMA)]^+$ (**3a,b**), in which five nitrogen donor centers from one molecule of PMAH are coordinated to copper (Figure 1). Coordination of the deprotonated amido N to the metal center in $[Cu(PMA)]^+$ is definitely assisted by the presence of acetate in the reaction mixture since the characteristic turquoise color of $[Cu(PMA)]^+$ is not observed when $Cu(ClO_4)_2$ or $Cu(BF_4)_2$ is used as the source of copper. Addition of sodium acetate (~2 equiv) to a reaction mixture containing $Cu(ClO_4)_2$ (or $Cu(BF_4)_2$) and PMAH in aqueous methanol, however, results in a color change from deep blue to turquoise, and on evaporation, crystals of **3b** (or **3a**) are obtained in moderate yield. Similar attempts indicate that, in aqueous solution, $[Cu(PMA)]^+$ can be synthesized from $Cu(ClO_4)_2$ and PMAH if the pH of the reaction mixture is adjusted from an initial value of ~5 to a final value of ~7. Coordination to metal ions is known to facilitate deprotonation of amide groups;[40] the pK_a for such a process in the case of PMAH and copper appears to be ~7.

The second complex $\{[Cu(PMAH)](ClO_4)_2 \cdot H_2O\}_2$ (**4**) is obtained by slow evaporation of a mixture of $Cu(ClO_4)_2$ and PMAH (ratio 1:1) in aqueous methanol. As described in the "structure" section, PMAH exhibits a very different mode of coordination in **4**. In a centrosymmetric dimeric structure (Figure 2), the ligand employs three nitrogens (the primary and secondary amine N's, one pyrimidine N) to bind one copper while the imidazole nitrogen is bonded to the other copper center. The amide function is not involved in coordination and remains in the protonated form. The latter fact is clearly evident in the IR spectrum of **4**, where ν_{CO} appears at 1660 cm^{-1}, a position that is very close to that exhibited by the free ligand (1666 cm^{-1}). $[Cu(PMA)]^+$, on the other hand, displays ν_{CO} at 1600 cm^{-1} due to the fact that substitution of an amide proton by a metal ion lowers the double-bond character in the C–O bond.[40]

An apparent pH value of ~4 is recorded for the deep blue reaction mixture from which **4** is isolated. It is evident that in such weakly acidic solution, the five donor centers of PMAH do not participate in coordination; only the two amine nitrogens and one ring nitrogen from the pyrimidine are attached to the metal. The amide group, in the protonated form, is not a good ligand[40] and refrains from ligation to copper. As a consequence of amide group not being involved in coordination, the imidazole nitrogen also fails to coordinate to the same copper center due to the inherent instability of very large chelate rings. Thus, the entire histamine tail of PMAH remains unbound. The final result is, therefore, the formation of a copper-containing species that includes three nitrogen atoms (two amine N's and one pyrimidine N) and most probably one oxygen atom (water molecule) in the basal coordination plane of the metal. Axial ligation by water molecule(s) is not ruled out. The complex **4** presumably results from dimerization of this species with concomitant loss of water molecules from the coordination sphere. Preferential crystallization of the dimer from concentrated solutions allows successful isolation of this important intermediate.

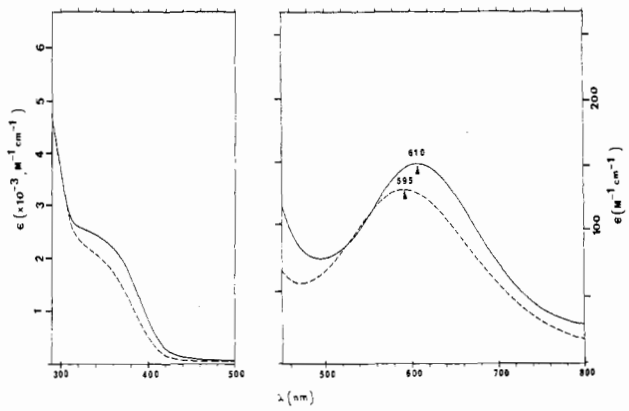

Figure 3. Electronic absorption spectra of **3** (solid line) and **4** (broken line) in Me_2SO solutions.

It has been reported previously[25b] that, at low pH (~1.5), formation of Cu(II)–BLM probably involves the pyrimidine and the secondary amine nitrogen; two water molecules complete the basal-plane coordination. The present study confirms this report. However, the same previous study concluded that in Cu(II)–BLM further coordination of the peptide nitrogen (deprotonated) of the histidine residue and the histidine imidazole nitrogen occurs at pH 2.5. Unless the deprotonation of this particular amide group in BLM is augmented by steric and/or some unknown interaction, the present work suggests that such deprotonation is likely to occur at higher pH. Our results also differ from the previous report[25b] in that the apical ligation of the α-amino nitrogen of β-aminoalanine to copper in Cu(II)–BLM is complete around pH 3; reproducible synthesis and structural characterization of **4** indicate that, at lower pH (~3), the amine group coordinates in the basal plane of copper. It should be noted that, in case of a partially ligated copper(II) complex (as in **4**), the preference for basal over apical coordination by the NH_2 end of PMAH (and also of BLM) is expected because of the Jahn–Teller effect.

Complete chelation by PMAH to *one* copper(II) center occurs around pH 7. As described in the Experimental Section, addition of bases (enough to raise the pH to 7) to the deep blue solution of **4** brings about a color change to turquoise, indicating the formation of **3**.[41] The transformation **4** → **3** is rather remarkable, since it requires a significant extent of reorganization in the coordination sphere of the metal ion. In **4**, the amide group and the histamine imidazole of PMAH are not involved in coordination. However, as the pH is adjusted to ~7, the amide group loses its proton[42] and the affinity of the amido nitrogen (N3) toward copper increases considerably. In order to allow ligation of N3 to copper, the pyrimidine ring exchanges its donor nitrogen from N4 (in **4**) to N5 (in **3**). Once N5 and N3 are bound to copper, the imidazole ring nitrogen N1 is also conveniently positioned for coordination to the same metal center. Since the deprotonated amido nitrogen (N3) and the imidazole nitrogen (N1) are both strong donors[40] and therefore prefer coordination in the basal plane, the primary amine group is forced to occupy the apical position. This completes the formation of $[Cu(PMA)]^+$ (**3**). The reverse transformation, namely **3** → **4**, is achieved in acidic solutions (pH ~4) and presumably follows similar steps but in reverse order (vide infra).

(38) Ou, C. C.; Miskowski, V. M.; Lalancette, R. A.; Potenza, J. A.; Schugar, H. J. *Inorg. Chem.* **1976**, *15*, 3157 and references cited therein.
(39) Sundberg, R. J.; Martin, R. B. *Chem. Rev.* **1974**, *74*, 471.
(40) Sigel, H.; Martin, R. B. *Chem. Rev.* **1982**, *82*, 385.
(41) For the sake of brevity, $[Cu(PMA)]^+$ is denoted as **3** hereafter.
(42) In presence of bivalent copper, values for the pK_a of the amide group of several dipeptides of histidine have been reported to lie in the range 5–7.[40]

Table IV. Electronic Spectral Data for $[Cu(PMA)]^+$ (**3**)[a] and $\{[Cu(PMAH)](ClO_4)_2 \cdot H_2O\}_2$ (**4**)[b]

solvent	λ_{max}, nm (ϵ, M^{-1} cm^{-1})[c]	
	complex **3**	complex **4**
H_2O (pH 7)	612 (130), 330 sh (3000), 290 sh (5100)	612 (130), 330 sh (3100), 290 (5200)
DMF	610 (150), 340 sh (2700)	605 (120), 340 sh (2600)
DMSO	610 (155), 340 sh (2700)	595 (140), 340 sh (2500)

[a] The spectral parameters of **3a** and **3b** are identical. [b] For Cu(II)–BLM in water (pH ~7) (λ_{max}, nm (ϵ)): 595 (120), 292 (17 400) (bithiazole absorption), 320 sh (4000), 250 (23 000).[46] Cu(II)–P-3A exhibits a d–d band at 625 nm (ϵ = 125) in water (pH 7).[10,11] [c] Values are quoted per Cu atom.

Electronic Absorption Spectra. The absorption spectra of **3**[43] and **4** in Me_2SO are shown in Figure 3, while the peak positions and extinction coefficients in various solvents are presented in Table IV. In each case, a single broad d–d band is observed in the visible region. Close inspection of the spectral parameters in Table IV reveals certain clues related to the solution structures of these two copper complexes. The enhanced intensity in the case of **3** is suggestive of distortion of the coordination sphere caused by steric constraints in the five-membered chelate rings. Since the position of the visible band maximum (λ_{max}) of **3** remains unchanged with change of solvent (Table IV), axial ligation by solvent molecule(s) to copper in $[Cu(PMA)]^+$ seems unlikely.[44] In contrast, participation of solvent molecules in axial coordination is evident in the shift of λ_{max} for **4** in various solvents.

When crystals of **4** are dissolved in water, the pH of the solution drops; the pH of a 1.5 mM solution of **4** in water is ~5. Following adjustment of the pH to 7, the solution exhibits an absorption spectrum (Table IV) which is identical to that of **3** (also at pH 7). Clearly, **4** is converted into **3** in dilute aqueous solution at neutral pH. Solvent-assisted deprotonation of the amide group of the partially ligated PMAH in **4** appears to be rather facile in water; in solvents like Me_2SO, **4** → **3** conversion hardly proceeds to the right. Spectroscopic studies, however, demonstrate that addition of a stoichiometric amount of a base like triethylamine (or water, >50%) to a solution of **4** in Me_2SO facilitates the **4** → **3** conversion. Addition of 1 equiv of $HClO_4$ to a solution of **3** in Me_2SO brings about the reverse, i.e. **3** → **4**, transformation.

Examination of Table IV calls for additional discussion on the position of the absorption band maximum of Cu(II)–BLM in water. When the spectral parameters of **3** in aqueous solution (pH 7) are compared with those of Cu(II)–BLM[45] and Cu(II)–P-3A under similar conditions,[10,11] it immediately becomes evident that even though the structure of the first coordination sphere around copper is expected to be the same in these three complexes, the λ_{max} values are distinctly different. It is quite possible that the λ_{max} values in such cases are very susceptible to minor distortions in the coordination sphere of copper caused by steric crowding in the organic framework, which follows the order BLM > P-3A > PMAH. Small variations in the ligand-field strength of the pyrimidine nitrogen (N5) due to different sets of substituents on the pyrimidine ring could also be responsible for the observed shift in the λ_{max} values. Since changes in axial ligation in tetragonal or square-pyramidal copper(II) complexes bring about shifts of the λ_{max} values for the d–d bands,[44] different axial donor(s) in solution might be responsible for this anomaly as well.[48]

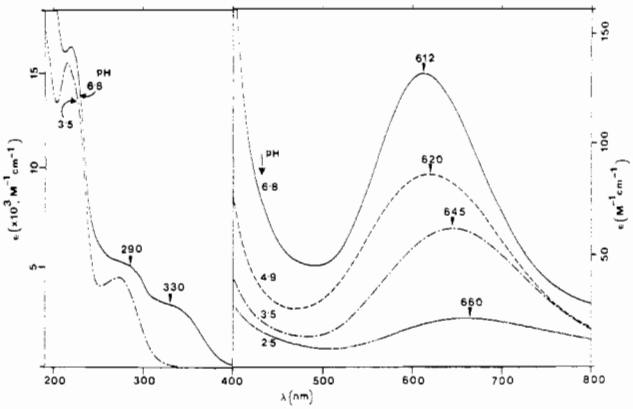

Figure 4. Electronic absorption spectra of **3** in water as a function of pH. On the higher energy side, only two spectra are shown to avoid overlapping traces.

Additional studies are definitely needed to account for the differences in the λ_{max} values as shown in Table IV.

The features in the 350–250-nm range of the electronic spectrum of **3** (Table IV) arise from absorption by the organic chromophores of the ligand. The 275-nm band maximum of PMAH shifts to lower energy (290 nm) on coordination to copper. Similar behavior has been observed with BLM.[47] In addition, the shoulder at 330 nm (ϵ = 3000 M^{-1} cm^{-1}) is assigned to a $d\pi \rightarrow \pi^*$ metal-to-ligand charge-transfer transition involving the pyrimidine ring.[18] In Cu(II)–BLM, this absorption appears at 327 nm as a shoulder on the intense bithiazole peak.[46] In summary, the 350–250-nm portion of the absorption spectrum of **3** closely resembles the corresponding section of the Cu(II)–BLM spectrum except for the bithiazole absorption.

Changes in the absorption spectrum of **3** with decreasing pH demonstrate the stepwise displacement of the various donor groups from the coordination sphere of copper in $[Cu(PMA)]^+$. Shown in Figure 4 are the absorption spectra of **3** in water as a function of pH. Increasing acidity brings about a decrease in the intensity of the visible absorption band of **3**, and at the same time the band maximum shifts to lower energy. Very similar observations have been noted with Cu(II)–BLM.[24,25] In the case of **3**, the first significant drop in intensity and shift of band maximum are observed when the pH is lowered below 5. Since $[Cu(PMAH)]^{2+}$ (**4**) is converted into $[Cu(PMA)]^+$ (**3**) above pH ~6, the deprotonated amido nitrogen (N3) of **3** appears to be the first donor site to be protonated and the red shift of the visible band maximum is consistent with the loss of the strong-field amido N (and possibly the imidazole nitrogen N1) from the coordination sphere of copper. As the pH is lowered further to ~3.5, the pyrimidine nitrogen (N5) gets detached from the metal center and is clearly evidenced by the loss of the 350-nm band (Figure 4), which is assigned to a $d\pi \rightarrow \pi^*$ metal-to-ligand charge-transfer transition involving the pyrimidine ring.[18,46] At pH 2.5, the aqueous solution of **3** exhibits a broad visible band with maximum at 660 nm (ϵ = 24 M^{-1} cm^{-1}). This is reminiscent of the absorption spectrum of $[Cu(NH_3)_2(H_2O)_4]^{2+}$ [49] and indicates that, at low pH, only the primary and secondary amine nitrogens of PMAH are coordinated to copper. Interesting to note is that this sequence of events is in complete agreement with the observations described under the "synthesis and interconversion" section.

Chelation by PMAH to copper is expected to afford two stereoisomers of opposite chirality. Since **3** crystallizes in a centric group (Table I), it is clear that both enantiomers are present in the crystal lattice.[50] Indeed, no circular dichroism (CD) activity was recorded with solutions of **3** in water or Me_2SO. Also, no dichroic effect was observed with $[Cu(PMA)]^+$ generated in situ by mixing copper(II) acetate with PMAH in methanol. Absence

(43) Spectral parameters of **3a** and **3b** are identical.
(44) Belford, R. L.; Calvin, M.; Belford, G. *J. Chem. Phys.* **1957**, *26*, 1165.
(45) With Cu(II)–BLM, different λ_{max} values have been reported: 610 nm (ϵ = 95 M^{-1} cm^{-1}),[24] 605 nm (ϵ = 100 M^{-1} cm^{-1}),[25b] and 595 nm (ϵ = 120 M^{-1} cm^{-1}).[46] At least three groups[10,11,46,47] have reported the last set of numbers consistently and hence the combination 595 nm (120) is included in Table IV as the value for Cu(II)–BLM.
(46) Dabrowiak, J. C.; Greenaway, F. T.; Longo, W. E.; Van Husen, M.; Crooke, S. T. *Biochim. Biophys. Acta* **1978**, *517*, 517.
(47) Takita, T. In ref 8a, p 156.
(48) Interestingly, Cu(II)–deglycoBLM exhibits its d–d band maximum at 610 nm (ϵ = 130 M^{-1} cm^{-1}).[10,11] Whether this indicates that the sugar moiety is involved in coordination to copper in Cu(II)–BLM (λ_{max} = 595 nm, ϵ = 120 M^{-1} cm^{-1}) or not is unclear at the present time.
(49) Cotton, F. A.; Wilkinson, G. In *Advanced Inorganic Chemistry*, 5th ed.; Wiley: New York, 1988; p 770.
(50) Glusker, J. P.; Trueblood, K. N. In *Crystal Structure Analysis, A Primer*, 2nd ed.; Oxford: New York, 1985; p 99.

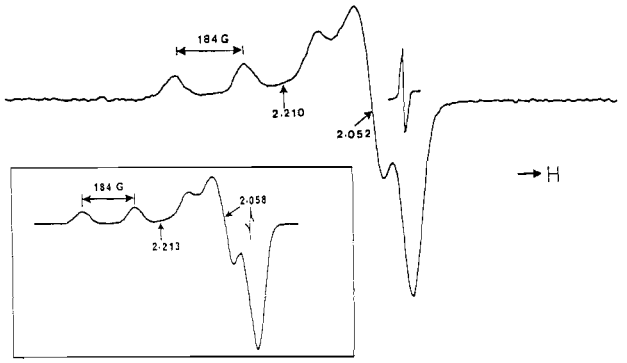

Figure 5. X-Band EPR spectrum (120 K) of $[Cu(PMA)]^+$ (**3**) in aqueous glycerol (7:3 v/v). Inset: X-band EPR spectrum (80 K) of Cu(II)–BLM in aqueous solution (1 mM) at pH 7.2. Selected g and $A_\parallel$ values are indicated. Spectrometer settings: microwave frequency, 9.19 GHz; microwave power, 10 mW; modulation frequency, 100 kHz; modulation amplitude, 2.0 G.

Table V. EPR Parameters

complex	$g_\parallel$	$g_\perp$	$A_\parallel$, G
$[Cu(PMA)]^+$ (**3**)[a]			
aq glycerol (7:3), 120 K	2.210	2.052	184
DMF, 120 K	2.220	2.060	184
$\{[Cu(PMAH)](ClO_4)_2 \cdot H_2O\}_2$ (**4**)			
DMF, 120 K	2.237	2.045	194
Cu(II)–BLM[b]	2.211	2.055	183
Cu(II)–BLM[c]	2.213	2.058	184
Cu(II)–P-3A[b]	2.214	2.133, 2.078	167.3
Cu(II)–PYML-1[b]	2.206	2.048	179.4
Cu(II)–AMPHIS[d]	2.204	2.050	177.5

[a] The EPR parameters of **3a** and **3b** are identical. [b] Reference 11. [c] Conditions: aqueous solution, pH 7.2, 80 K. [d] Reference 17b.

of CD features has been reported for the analogue Cu(II)–PEML.[10,11] Unlike BLM analogues like PYML[10,11] and AMPHIS[17] (the copper complexes of both ligands exhibit CD spectra), PMAH has fewer substituents on the two side chains. It is therefore possible that, on steric grounds, no specific preference toward a particular stereoisomer exists in the present case.

EPR Spectra. Cu(II)–BLM exhibits an axial EPR spectrum (inset, Figure 5) that is typical of a monomeric tetragonal Cu(II) complex with a $d_{x^2-y^2}$ ground-state doublet. As shown in Figure 5, the EPR spectrum of $[Cu(PMA)]^+$ (**3**) in aqueous glycerol glass (120 K)[51] resembles the Cu(II)–BLM spectrum very closely. The spectral parameters of these two complexes, collected in Table V, are practically identical. This confirms a square-pyramidal N_5 coordination around copper in aqueous solution of Cu(II)–BLM at physiological pH.

No well-resolved superhyperfine coupling to the nitrogen donors has been detected in the EPR spectra of the synthetic analogues of Cu(II)–BLM.[10,11,17] In this regard, **3** is no exception. In spite of this fact, certain features of the coordination structure can be extracted from Table V in which the EPR parameters of other synthetic analogues and Cu(II)–P-3A are also included. It is interesting to note that a closer match in spectral parameters exists between Cu(II)–BLM and **3** rather than the former and Cu(II)–P-3A (Tables IV and V). This is somewhat surprising since the metal-chelating locus of P-3A is identical with that of BLM except for one methyl group on the pyrimidine ring. Overall, BLM is a more complex molecule than P-3A. Nevertheless, Cu(II)–P-3A exhibits a rhombic EPR spectrum, which indicates that the coordination of sphere of copper in Cu(II)–P-3A is less symmetric as compared to the one present in Cu(II)–BLM.[11] The smaller value of $A_\parallel$ (167 G) observed with Cu(II)–P-3A also suggests the existence of a more distorted coordination sphere around copper in this complex.[52] At present, the reason for this distortion in

(51) Addition of glycerol to the aqueous solutions improves the quality of the glass. The electronic spectrum of **3** in 7:3 (v/v) aqueous glycerol is identical with that in water only.

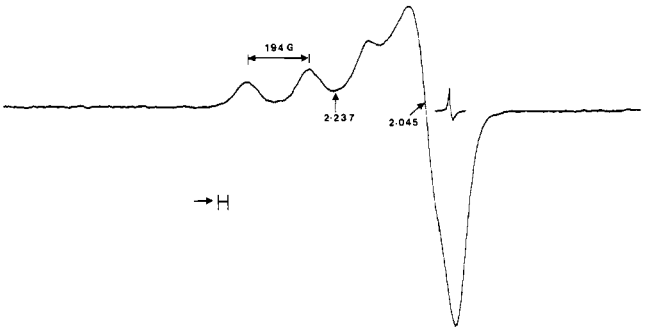

Figure 6. X-Band EPR spectrum (120 K) of **4** in DMF solution. Instrument settings: same as in Figure 4.

Cu(II)–P-3A is unknown. In contrast, the spectral characteristics of **3** are very similar to those of Cu(II)–BLM, and hence **3** is a better representation of the coordination structure of copper in Cu(II)–BLM. "Typical" Cu(II)–BLM spectra have also been obtained for PYML-1[10,11] and AMPHIS[17] analogues. However, both these analogues, unlike BLM, contain a pyridine ring in their organic framework. The claim that **3** is by far the closest mimic of Cu(II)–BLM therefore remains as a legitimate one.

Figure 6 displays the EPR spectrum of **4** in DMF glass (120 K). The spectrum clearly demonstrates that the dimeric structure **4**, as observed in the crystalline state (Figure 2), dissociates in solution, and the observed spectrum is that of the monomeric Cu(II) species with PMAH partially ligated to the metal center. As described in a previous section, only three of the five nitrogen donor centers of PMAH are bonded to copper in this presumably tetragonal complex while the remaining coordination sites are occupied by solvent molecules. This monomeric intermediate with partially ligated PMAH can be easily distinguished from **3** (i.e., the structure in which chelation by PMAH to copper is complete) by the absence of the inflection around $g = 2$ in its EPR spectrum (compare Figures 5 and 6). Also, a difference in the ligand set and/or the lack of steric constraint in the coordination sphere of copper in this intermediate structure gives rise to a higher $A_\parallel$ value (194 G, Table V). That **4** is converted into **3** in aqueous solution has also been confirmed by EPR spectroscopy.

Electrochemical, Spin-Trapping, and DNA Cleavage Experiments. The redox properties of **3** in aqueous and nonaqueous solutions have been studied by cyclic voltammetry and differential-pulse polarography. In aqueous phosphate buffer (pH 7), **3** is quasi-reversibly reduced on a hanging-mercury-drop electrode (HMDE) at $E_p = -0.24$ V (vs Ag/AgCl). The peak potential (E_p) for reduction shifts to −0.27 V (vs Ag/AgCl) in DMF. Voltammetric characteristics at a dropping-mercury electrode (DME) and a glassy-carbon electrode are practically identical with those at a HMDE. The E_p value of **3** is close to the half-wave potential ($E_{1/2}$) reported for the analogue Cu(II)–PEML (−0.26 V)[10,11] but more positive as compared to the $E_{1/2}$ value of Cu(II)–BLM (−0.52 V).[10,11,53] Structural strain in the five-membered chelate rings in Cu(II)–PEML has been attributed to the ease of reduction of the copper center.[10,11] The same effect might account for the relatively high reduction potential of **3**. The discrepancy in redox behavior between **3** and Cu(II)–BLM should, however, be regarded as a plus since the higher reduction potential of **3** allows this analogue to form free radicals more efficiently and to inflict more damage to DNA (vide infra).

Initial investigations[54] and a recent report[55] have suggested that Cu(II)–BLM in the presence of DTT or β-mercaptoethanol fails to degrade DNA. However, careful studies[56] have established

(52) Miyoshi, K.; Tanaka, H.; Kimura, E.; Tsuboyama, S.; Murata, S.; Shimizu, H.; Ishizu, K. *Inorg. Chim. Acta* **1983**, *78*, 23.
(53) Ishizu, K.; Murata, S.; Miyoshi, K.; Sugiura, Y.; Takita, T.; Umezawa, H. *J. Antibiot.* **1981**, *34*, 994.
(54) (a) Shirakawa, I.; Azegami, M.; Sin-ichi, I.; Umezawa, H. *J. Antibiot.* **1971**, *24*, 761. (b) Antholine, W. E.; Solaiman, D.; Saryan, L. A.; Petering, D. H. *J. Inorg. Biochem.* **1982**, *17*, 75.
(55) Suzuki, T.; Kuwahara, J.; Sugiura, Y. *Biochemistry* **1985**, *24*, 4719.

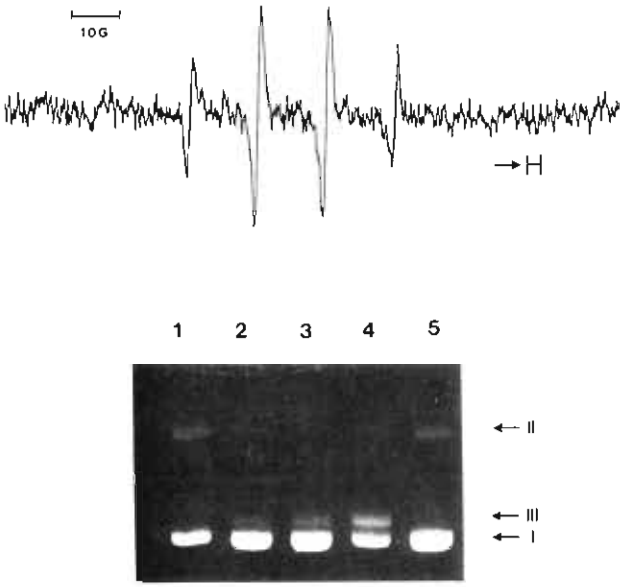

Figure 7. (Top) ESR spectrum of the DMPO–OH spin adduct at 20 °C (for experimental conditions see "other physical measurements" section). Instrument settings for the spin-trapping experiment: microwave power, 10 mW; field set 3360 G; modulation frequency, 100 kHz; modulation amplitude, 1 G; time constant, 0.3 s; scan time, 6 min; receiver gain, 1×10^5. (Bottom) Plasmid (ϕX174 rf) DNA cleavage experiment with **3** in phosphate buffer (3 mM, pH 7.5): lane 1, DNA (1 μg) + $CuSO_4$ (1×10^{-5} M) + DTT + O_2; lane 2, DNA + **3** (1×10^{-6} M) + DTT + O_2; lane 3, DNA + **3** (1×10^{-5} M) + DTT + O_2; lane 4, DNA + **3** (1×10^{-4} M) + DTT + O_2; lane 5, DNA + DTT + O_2.

that copper–BLM does induce DNA strand breaks in the presence of DTT and dioxygen. The controversy apparently resulted from the facts that, despite no direct DNA cleavage activity, Cu(II)–BLM is slowly reduced to Cu(I)–BLM by DTT[57] and Cu(I)–BLM is readily oxidized by dioxygen with concomitant generation of oxygen-based radicals like $^{\bullet}OH$,[58] which inflict significant damage to DNA. Since the spectral characteristics of **3** closely mimic those of Cu(II)–BLM, spin-trapping experiments were attempted to study production of oxygen-based radical(s) by **3** in the presence of DTT and dioxygen. In phosphate buffer (pH 7), the typical turquoise color of **3** is bleached upon addition of DTT and the color returns when oxygen is bubbled through the solution for ca. 1 min. These observations confirm that **3** is reduced by DTT to a Cu(I) species that can be reoxidized upon oxygenation. When excess DMPO is present in such reaction mixtures, the characteristic ESR spectrum of the spin adduct of the $^{\bullet}OH$ radical is recorded (Figure 7).[59] The ESR pattern and the parameters are as follows: 1:2:2:1 quartet, $g = 2.0060$, $A_N = A_H = 15$ G. This result clearly demonstrates that $^{\bullet}OH$ radicals are generated by the $[Cu(PMA)]^+$–DTT–O_2 system.

Studies on the nature and the extent of DNA damage by the $[Cu(PMA)]^+$–DTT–O_2 system have yielded encouraging results. When supercoiled covalently closed-circular plasmid (pBR 322 or the replicative form of ϕX174) DNA (type I) is incubated with micro- to submillimolar solution of **3** in phosphate buffer (pH 7) in the presence of DTT and oxygen, appreciable amounts of nicked circular (type II) and linear (type III) DNA molecules are formed within a short time (Figure 7). The latter two forms of DNA molecules presumably result from the single- and double-strand breaks in type I DNA following attack by the $^{\bullet}OH$ radical.[1] In absence of **3**, no DNA cleavage activity is noted under similar reaction conditions (lane 5, Figure 7) and control experiments with $CuSO_4$ (lane 1, Figure 7) indicate that the extent of DNA strand breaks is minimal. Clearly, the anticipated oxygen activation by **3** is detected. Densitometric measurements on the agarose gels reveal an interesting characteristic of the DNA cleavage reaction by **3**. In a typical experiment under reaction conditions as mentioned in the Experimental Section, 10^{-5} M $CuSO_4$ afforded 17% type II and no type III product. In contrast, incubation with **3** resulted in the following product distribution (concentration of **3**, % type II and % type III normalized to a total of 100%): 1×10^{-6} M, 7.5, 19.7; 1×10^{-5} M, 8.1, 22; 1×10^{-4} M, 9.2, 35.5. DTT alone (5 mM) generated 16% type II within the same time period. It is thus apparent that **3** induces more double-strand breaks. Given the low probability of bimolecular collisions between the highly reactive radical(s) and DNA in solution and the fact that **3** is devoid of any DNA-intercalating group like the bithiazole moiety of BLM, the DNA cleavage activity of **3** is specially noticeable. The relatively high Fe(III)/Fe(II) redox potential of the BLM–iron complex is believed to be responsible for the capacity to effect rapid DNA degradation.[55,60] It is quite probable that the high redox potential allows facile DTT reduction of **3** to Cu(I) species, which upon oxygenation produces the $^{\bullet}OH$ radical in sufficient amount to cause DNA strand scission.[61] Additional studies toward elucidation of the DNA cleavage reaction by **3** are in progress, and the results will be reported elsewhere.

Summary and Conclusion

The following are the principal results and conclusions of this investigation:

(i) PMAH (**2**), a synthetic analogue of the metal-chelating portion of the antitumor drug bleomycin (BLM, **1**) has been synthesized. Unlike the previous ones, this analogue contains a pyrimidine ring in the organic framework.

(ii) The copper(II) complex $[Cu(PMA)]^+$ (**3**) in which PMA^- is coordinated to the metal ion through five N donor centers has been isolated and characterized. The crystal structures of two different salts of $[Cu(PMA)]^+$ (**3a**,**b**) unequivocally establish the proposed coordination sphere of Cu in Cu(II)–BLM at the physiological pH. Prior to this work, no synthetic analogue of M–BLM had been isolated in the crystalline form.

(iii) Structural and spectroscopic studies indicate that, in **3**, the sixth coordination site on copper remains vacant both in solid state and in solution. Since BLM is a more crowded ligand, it is quite probable that, in Cu(II)–BLM, the sixth site on copper is free and is only accessible to small molecules.

(iv) The crystal structure of a second copper(II) complex of PMAH, namely **4**, has also been determined. This complex is isolated at slightly acidic pH and is indeed an intermediate in the process of formation of **3**. In **4**, PMAH is partially coordinated to copper. The two complexes (**3**, **4**) are interconvertible.

(v) Reproducible synthesis of **4** confirms the fact that in aqueous solution at low pH the primary and the secondary amine nitrogens of the β-aminoalanine moiety of BLM as well as one nitrogen from the pyrimidine ring are coordinated to copper. It also appears that the amide nitrogen between the pyrimidine and the imidazole rings of BLM does not participate in coordination below pH $\approx$6. Clearly, transformation of the low-pH form of Cu(II)–BLM to the one containing a square-pyramidal CuN_5 chromophore (observed at physiological pH) requires reorganization of the donor centers around copper to a great extent. The present work suggests that such reorganization in the coordination sphere of copper might be rather facile at neutral pH. The striking changes in the CD spectrum of Cu(II)–BLM with pH in the range pH 3–5[25b] could

(56) (a) Ehrenfeld, G. M.; Shipley, J. B.; Heimbrook, D. C.; Sugiyama, H.; Long, E. C.; van Boom, J. H.; van der Marel, G. A.; Oppenheimer, N. J.; Hecht, S. M. *Biochemistry* **1987**, *26*, 931. (b) Ehrenfeld, G. M.; Rodriguez, L. O.; Hecht, S. M.; Chang, C.; Basus, V. J.; Oppenheimer, N. J. *Biochemistry* **1985**, *24*, 81.

(57) (a) Freedman, J. H.; Horwitz, S. B.; Peisach, J. *Biochemistry* **1982**, *21*, 2203. (b) Takahashi, K.; Yoshioka, O.; Matsuda, A.; Umezawa, H. *J. Antibiot.* **1977**, *30*, 861.

(58) (a) Oppenheimer, N. J.; Chang, C.; Rodriguez, L. O.; Hecht, S. M. *J. Biol. Chem.* **1981**, *256*, 1514. (b) Sugiura, Y. *Biochem. Biophys. Res. Commun.* **1979**, *90*, 375.

(59) Mottley, C.; Connor, H. D.; Mason, R. P. *Biochem. Biophys. Res. Commun.* **1986**, *141*, 622.

(60) Melnyk, D. L.; Horowitz, S. B.; Peisach, J. *Biochemistry* **1981**, *20*, 5327.

(61) That no iron impurity in any reagent is responsible for the observed DNA strand scission has been checked by atomic absorption spectroscopy.

be indicative of reorganization of the donor centers around copper in Cu(II)-BLM.

(vi) In aqueous phosphate buffer (pH 7), **3** is reduced at a relatively high potential (-0.27 V vs Ag/AgCl). This allows facile DTT reduction of **3** to Cu(I) species that upon oxygenation produces the •OH radical. The $[Cu(PMA)]^+$-DTT-O_2 system induces significant amounts of double-strand breaks in plasmid DNA.

Acknowledgment. Financial support from the donors of the Petroleum Research Fund, administered by the American Chemical Society, at UCSC and from the NSERC of Canada at the University of Windsor is gratefully acknowledged. Part of this research was also supported by a grant from the Cancer Research Coordinating Committee of UC.

Supplementary Material Available: Crystal structure data for **3b** and **4** including thermal parameters for non-hydrogen atoms (Table S1), positional parameters for the hydrogen atoms (Table S2), and selected bond distances and angles associated with the perchlorate groups (Table S3) (5 pages); observed and calculated structure factors (Table S4) (11 pages). Ordering information is given on any current masthead page.

Contribution from Salutar, Inc., 428 Oakmead Parkway, Sunnyvale, California 94086, and the Department of Chemistry, University of California, Berkeley, California 94720

Manganese(II) *N,N'*-Dipyridoxylethylenediamine-*N,N'*-diacetate 5,5'-Bis(phosphate). Synthesis and Characterization of a Paramagnetic Chelate for Magnetic Resonance Imaging Enhancement

Scott M. Rocklage,*,† William P. Cacheris,† Steven C. Quay,† F. Ekkehardt Hahn,‡ and Kenneth N. Raymond‡

Received September 29, 1988

The synthesis and characterization of the new ligand *N,N'*-dipyridoxylethylenediamine-*N,N'*-diacetic acid 5,5'-bis(phosphate) (DPDP, for dipyridoxal diphosphate) are described. The solution equilibrium properties of DPDP and the Mn(II), Zn(II), Cu(II), and Fe(III) complexes have been determined. log K_{ML} values are 15.10, 18.95, 22.08, and 33.52 for $MnDPDP^{6-}$, $ZnDPDP^{6-}$, $CuDPDP^{6-}$, and $FeDPDP^{5-}$, respectively. Crystals of the salt $CaNa_2MnC_{22}H_{26}N_4O_{14}P_2 \cdot 21H_2O$ (**1**) are monoclinic, space group $C2/c$ (No. 15), with a = 24.490 (3) Å, b = 14.440 (2) Å, c = 30.703 (4) Å, β = 112.747(12)°, and Z = 8. The asymmetric unit contains 1 MnDPDP anion, 1 calcium cation, 2 sodium cations, and 21 water molecules. The manganese(II) oxidation state was confirmed by the stoichiometry, by the Mn-O1, Mn-O8, Mn-N2, and Mn-N4 bond distances, and by magnetic susceptibility measurements. In vivo applications of MnDPDP for magnetic resonance imaging enhancement are discussed.

Introduction

We recently reported the structural and thermodynamic characterization of manganese(II) *N,N'*-dipyridoxylethylenediamine-*N,N'*-diacetate, MnPLED.[1] This complex represented an example of a Mn(II) hexadentate chelate that is stable to hydrolysis at neutral pH. This was part of our research program aimed at the preparation and characterization of paramagnetic chelates containing biologically relevant organic moieties for NMR imaging contrast enhancement, in which we are now investigating the coordination chemistry of ligands derived from pyridoxal 5-phosphate (PLP), the coenzyme of vitamin B_6. MnPLED was found to have a thermodynamic stability constant slightly lower than that of MnEDTA (log K of 12.56 vs 13.95) and to have limited aqueous solubility (<50 mM). For these reasons derivatives have been sought that would overcome these deficiencies.

Pyridoxal 5-phosphate containing enzymes participate in the deamination, decarboxylation, transamination, racemization, and transsulfurization of amino acids and in the metabolism of fats and carbohydrates.[2] A number of studies have demonstrated that nonenzymatic transamination is catalyzed by certain metal ions in ternary model systems containing an amino acid, carbonyl compound, and metal ion.[3-5] A general mechanism for PLP-catalyzed reactions proposed by Metzler et al.[6] is the formation of an intermediate Schiff base from PLP and an amino acid. Subsequent work has shown that the metal ion stabilizes the aldimine and ketamine Schiff base forms by chelation;[7-10] NMR studies of binary PLP-metal ion systems with paramagnetic shift agents have demonstrated coordination of metal ions via the phosphate moiety with limited participation by the aldehyde.[11-13]

The novel ligand described in this paper, *N,N'*-dipyridoxylethylenediamine-*N,N'*-diacetic acid 5,5'-bis(phosphate), forms stable, highly water-soluble hexadentate chelates involving the PLP hydroxy groups. Herein, we report the synthesis and characterization of this new ligand and the solution equilibrium properties with Mn(II), Cu(II), Zn(II), and Fe(III) ions.

Experimental Section

Synthesis of *N,N'*-Dipyridoxylethylenediimine 5,5'-Bis(phosphate). A 12-L three-neck round-bottom flask fitted with a mechanical stirrer was charged with 530.8 g (2.0 mol) of pyridoxal 5-phosphate and 2.5 L of CH_3OH. The mixture was stirred while 800 mL of 5 N NaOH was added. When a homogeneous yellow solution was obtained (in ca. 15 min), 67 mL (1.0 mol) of 1,2-ethylenediamine was added and a bright yellow precipitate of the bis(imine) formed immediately. The yellow slurry was stirred for 1 h and subsequently used without isolation for the next step.

Synthesis of *N,N'*-Dipyridoxylethylenediamine 5,5'-Bis(phosphate). The bis(imine) slurry from above was diluted with 2.5 L of water and

†Salutar, Inc.
‡University of California.

(1) Rocklage, S. M.; Sheffer, S. H.; Cacheris, W. P.; Quay, S. C.; Hahn, E. F.; Raymond, K. N. Structural and Thermodynamic Characterization of Manganese(II) *N,N'*-Dipyridoxylethylenediamine-*N,N'*-diacetate. *Inorg. Chem.* **1988**, *27*, 3530-3534.
(2) Dolphin, D.; Poulson, R.; Avramovic, O. Vitamin B6 Pyridoxal Phosphate, Chemical, Biochemical, and Medical Aspects. *Coenzymes and Cofactors*; Wiley-Interscience: New York, 1986; Vol. 1, Part B.
(3) Snell, E. E.; Fasella, P. M.; Braunstein, A.; Rossi-Fanelli, A. *Chemical and Biological Aspects of Pyridoxal Catalysis*; Macmillan Co.: New York, 1963; p 1.
(4) Bruice, T. C.; Benkovic, S. J. *Bioorganic Mechanisms*; W. A. Benjamin, Inc.: Reading, MA, 1966; Vol. 2, Chapter 8.
(5) Felty, W. L.; Ekstrom, C. G.; Leussing, D. L. *J. Am. Chem. Soc.* **1970**, *92*, 3006-3011.
(6) Metzler, D. E.; Ikawa, M.; Snell, E. E. *J. Am. Chem. Soc.* **1954**, *76*, 648.
(7) Langohr, M. F.; Martell, A. E. *J. Chem. Soc., Chem. Commun.* **1977**, 343.
(8) Langohr, M. F.; Martell, A. E.; Tatsumoto, K. *Inorg. Chim. Acta* **1985**, *108*, 105.
(9) Szpoganicz, B.; Martell, A. E. *Inorg. Chem.* **1986**, *25*, 327-332.
(10) Martell, A. E.; Taylor, P. *Inorg. Chem.* **1984**, *23*, 2734-2735.
(11) Narasinga Rao, B. N.; Ramakrishnan, C.; Balaram, P. *J. Biosci.* **1979**, *1*, 35-47.
(12) Viswanathan, T. S.; Swift, T. J. *Can. J. Chem.* **1979**, *57*, 1050-1055.
(13) Viswanathan, T. S.; Swift, T. J. *Can. J. Chem.* **1980**, *58*, 1118-1124.

0020-1669/89/1328-0477$01.50/0